Online Supporting Material

THE N-TERMINAL EXTENSION OF CARDIAC TROPONIN T STABILIZES THE BLOCKED-STATE OF CARDIAC THIN FILAMENT

Sampath K. Gollapudi, Ranganath Mamidi, Sri Lakshmi Mallampalli, and Murali Chandra*

Department of Veterinary and Comparative Anatomy, Pharmacology, and Physiology (VCAPP), Washington State University, Pullman, WA, USA

*Address correspondence to:
Murali Chandra, Ph.D, PO Box 646520, 210 Wegner Hall, Department of VCAPP, Washington State University, Pullman, WA-99164. Tel: +1 (509) 335-7561; Fax: +1 (509) 335-4650;
Email: murali@vetmed.wsu.edu

ONLINE SUPPORTING MATERIAL FOR EXPANDED MATERIALS AND METHODS

Preparation of detergent-skinned cardiac papillary muscle fiber bundles

Papillary muscle fiber bundles from NTG and TG mouse hearts were prepared using the procedure described previously (1,2). Briefly, mice were anaesthetized using isoflurane until they were deeply sedated. The depth of anesthesia was confirmed using a pedal withdrawal reflex. The hearts were quickly excised and placed into an ice-cold high relaxing solution of pCa 9.0 containing concentrations in mM of the following: 20 2, 3-butanedione monoxime, 50 N, N-bis (2-hydroxyethyl)-2-amino-ethane-sulfonic acid (BES), 30.83 Potassium propionate (K-propionate), 10 Sodium azide, 20 Ethylene glycol tetra-acetic acid (EGTA), 6.29 Magnesium chloride ($MgCl_2$), 6.09 Na_2ATP, 4 Benzamidine-HCl, and 1.0 of Dithiothreitol. The pH of the resulting solution was adjusted to 7.0 using KOH. Fresh stocks of the following protease inhibitors were also added to this solution in µM concentrations: 5 of Bestatin, 2 of E-64, 10 of Leupeptin, 1 of Pepstatin, and 200 of PMSF. Papillary muscle bundles were excised from the left ventricles of NTG and TG mouse hearts. Larger bundles were dissected into smaller bundles measuring 2-2.5 mm in length and 150 µm in width and thickness. These thinner fibers were subsequently skinned overnight at 4˚C in relaxing solution that contained 1% Triton X-100 (1).

pCa solutions

For pCa titrations, each fiber was bathed in different pCa solutions ranging from 9.0 to 4.3. The relaxing solution (pCa 9.0) contained the following (in mM concentrations): 50 BES, 5 NaN_3, 10 PEP, 10 EGTA, 0.024 $CaCl_2$, 6.87 $MgCl_2$, 5.83 Na_2ATP, and 51.14 K-propionate. The maximal Ca^{2+}-activating solution (pCa 4.3) contained the following (in mM concentrations): 50 BES, 5 NaN_3, 10 phosphoenol pyruvate, 10 EGTA, 10.11 $CaCl_2$, 6.61 $MgCl_2$, 5.95 Na_2ATP, and 31 K-propionate. In addition, pCa solutions contained 2 mg/ml pyruvate kinase, 0.2 mg/ml lactate dehydrogenase, along with a fresh cocktail of protease inhibitors (Leupeptin, Pepstatin, PMSF, A_2P_5, and Oligomycin). The reagent concentrations of all pCa solutions were calculated based on a program developed by Fabiato and Fabiato (3). The pH of each solution was adjusted to 7.0 using KOH.

Expression levels of sarcomeric proteins

To determine whether the level of other sarcomeric proteins was not altered in TG heart muscle, cardiac muscle proteins were analyzed on SDS-polyacrylamide gels (4). Muscle protein samples for gels were prepared as follows: ventricles from mouse hearts were frozen in liquid nitrogen and pulverized using a mortar and pestle. The tissue preparations were then dissolved using a muscle protein extraction buffer - 2.5% SDS, 10% glycerol, 50 mM tris base (pH 6.8 at 4ºC), 1 mM DTT, 1mM PMSF, 4 mM benzamidine HCl - that contained a fresh cocktail of phosphatase (PhosSTOP) and protease inhibitors (E-64, Leupeptin, and Bestatin). The total protein concentration of each sample was determined by Nanodrop (ND-1000, Nanodrop Products, Wilmington, DE) and the loading quantity of each preparation was standardized to 5 mg/ml by diluting it with gel loading buffer (125 mM Tris-HCl (pH 6.8), 20% glycerol, 2% SDS, 0.01% bromophenol blue, and 50 mM β-mercaptoethanol).

In our experiment, equal quantities of protein samples (25 μg of the sample) from NTG and TG mouse heart preparations were first run on a standard 8% mini SDS gel (30:0.8 of acrylamide:bis-acrylamide) to separate various sarcomeric proteins. The gel was then stained with Coomassie brilliant blue (R-250, Bio-rad Laboratories, Hercules, CA) to visualize the total protein content. Although an optimum separation of most proteins can be readily appreciated (Fig. S1 *A*), chimeric cTnT in the TG mouse heart preparation comigrated with tropomyosin. In an attempt to optimally resolve the separation between these two proteins, we prepared a large 12.5% SDS-gel (29:1.0 of acrylamide:bis-acrylamide) and ran the gel overnight. While we resolved the separation between chimeric cTnT and tropomyosin under these conditions, problem persisted in that the chimeric cTnT now comigrated with another sarcomeric protein. Although the expression of chimeric cTnT is clearly evident in the TG preparation, we could not quantify it because the chimeric cTnT comigrated with another unidentified sarcomeric protein. However, we were able to quantify the expression level of chimeric TnT using the Western blot (see Fig. 4 of the manuscript). The expression levels of other sarcomeric proteins (myosin heavy chain, myosin binding protein C, desmin, actin, tropomyosin, cardiac troponin I, myosin light chain 1, myosin light chain 2, and cardiac troponin C) appeared similar between NTG and TG cardiac muscle preparations.

Phosphorylation status in NTG and TG cardiac muscle preparations

To assess the phosphorylation status in NTG and TG heart muscle preparations, cardiac muscle proteins were analyzed on SDS-polyacrylamide gels (4). We used a standard SDS mini gel that contained 15% acrylamide, with a ratio of 29:1 (acrylamide:bisacrylamide). The gel was fixed and stained for phosphoproteins as described in the Invitrogen manual (Invitrogen Corporation, Carlsbad, CA). Fig. S2 shows that the phosphorylation status of sarcomeric proteins was similar in NTG and TG cardiac muscle preparations.

Measurement of ATPase activity in detergent-skinned cardiac muscle fibers

The ATPase activity, during steady-state isometric force, was measured using an assay described previously (5-7). In brief, a near UV light was projected through the muscle chamber. The muscle chamber was milled in an aluminum block and placed on top of a base that allowed water circulation for temperature control (20ºC). For efficient mixing, the solution in the bath was continuously stirred by means of motor-driven vibration of a membrane positioned at the base of the muscle chamber. The UV light was split 50:50 for intensity detection at 340 nm (sensitive to changes in NADH) and 400 nm (insensitive to changes in NADH) wavelengths. A change in the UV absorbance at 340 nm can be directly correlated to the oxidation of NADH (i.e., ATP usage) through enzymatically coupled reactions as follows: Pyruvate kinase converts phosphoenol pyruvate and the ADP generated from the steady-state ATP hydrolysis of actomyosin to ATP and pyruvate. Pyruvate is subsequently converted to lactate by lactate dehydrogenase in a reaction that is coupled to the oxidation of NADH to NAD^+. Light intensity of the beam at 400 nm served as the reference signal. After each recording, the UV absorbance signal of NADH was calibrated by multiple rapid injections of 25 pmol of ADP into the bathing solution, with a motor-controlled calibration pipette.

Rate of tension redevelopment (k_{tr})

The rate constant associated with the tension redevelopment, k_{tr}, was estimated using a modification to the original protocol developed by Brenner and Eisenberg (8). The resting SL of the detergent-skinned cardiac muscle fiber was set to either 1.9 or 2.3 µm in a relaxing solution (pCa 9.0) using laser diffraction technique. The overall fiber length, corresponding to the SL of either 1.9 µm or 2.3 µm, was recorded as the baseline muscle length (ML). The muscle fiber was then maximally activated in pCa 4.3. Once the fiber attained steady-state force, it was rapidly (0.5 ms) slackened by 10% of the baseline ML. The muscle fiber was then allowed to shorten briefly (25 ms) at the slackened length. The remaining bound cross-bridges (XBs) were mechanically detached by commanding the motor arm to rapidly swing past its original set point by 10% of the ML. The muscle fiber was then rapidly (0.5 ms) brought back to its original set point (corresponding to resting SL) and was allowed to redevelop force. Fig. S3 shows a representative sample of the force response (panel *A*) elicited by a detergent-skinned NTG mouse papillary muscle fiber in response to the large release-restretch length transient (panel *B*). k_{tr} was estimated by fitting a mono-exponential function to the force:

$$F = (F_{ss} - F_{res})\ (1 - e^{-k_{tr} t}) + F_{res} \qquad \text{(S1)}$$

where F_{ss} is the steady-state isometric force and F_{res} is the residual force from which the fiber starts to redevelop force.

Measurement of dynamic muscle fiber stiffness using step-like length perturbations

A series of step-like length perturbations (± 0.5, ± 1.0, ± 1.5, and ± 2.0% of the preset ML) was applied to maximally-activated detergent-skinned cardiac muscle fibers and the force responses were measured using the procedure described previously (9). Briefly, the ends of the muscle fiber were clipped using T-shape aluminum foil clips and the fiber was mounted between the force transducer (AE 801, The Sensor One Technologies, Sausalito, CA) and the servo motor (model 308B, The Aurora Scientific Inc., Aurora, Ontario, Canada). The fiber was then suspended into a chamber containing pCa 9.0 solution and the sarcomere length (SL) of the fiber was adjusted to either 1.9 µm or 2.3 µm. The fiber was then maximally activated and upon attainment of the steady-state in force, the motor arm was first commanded to quickly stretch the fiber by 0.5% of ML. The fiber was maintained at this increased length for 5 seconds to attain a new steady-state after which it was returned back to the baseline ML. This procedure was repeated for 1.0, 1.5, and 2.0% ML step magnitudes, and the corresponding force responses were measured. The force and the muscle length data were normalized to their respective isometric steady-state values just before the onset of step perturbations. A nonlinear recruitment-distortion (NLRD) model was fitted to the family of force responses elicited by the muscle fibers to various amplitude quick stretches and releases, in order to determine its linear and nonlinear contractile parameters. A short introduction on the NLRD model and the significance of the model parameters follows.

NLRD model formulation

The NLRD model comprises two components, a recruitment variable, $\eta(t)$, and a distortion variable, $x(t)$. $\eta(t)$ represents the net stiffness of the parallel stiffness elements, whereas, $x(t)$ represents the average elastic distortion of these elements. Thus, the net muscle force, $F(t)$, is determined by the product of recruitment and distortion variables as per the equation:

$$F(t) = \eta(t)\, x(t) \tag{S2}$$

Both $\eta(t)$ and $x(t)$ are dependent on the muscle length, $l(t)$, and their relationships with $l(t)$ are approximated using the first order differential equations, respectively,

$$\frac{d\eta(t)}{dt} = -b\,\eta(t) + \beta_0\left[l(t) - l_d\right] \tag{S3}$$

$$\frac{dx(t)}{dt} = -c\left[x(t) - x_0\right] + \frac{dl(t)}{dt} \tag{S4}$$

where b is recruitment rate constant, x_0 is the baseline isometric distortion imposed on the XB by the power stroke, β_0 is the scaling factor, l_d is the length at which no recruitment occurs, c is the distortion rate constant, and $dl(t)/dt$ is the rate of length change.

Using the formulation of the NLRD model (9), the immediate force response, F_1, and the new steady-state force response, F_{nss}, to change in ML, Δl were approximated as:

$$F_1 = 1 + \frac{\Delta l}{x_0} \tag{S5}$$

$$F_{nss} = 1 + \frac{\Delta l}{l - l_d} \tag{S6}$$

In the equations above, both F_1 and F_{nss} are normalized with respect to isometric steady-state force, F_{ss} ($= \eta_0 x_0$) and both are linear functions of Δl. Using Eqs. S5 & S6, the magnitude of instantaneous stiffness increase, E_D, and the magnitude of recruitment stiffness increase, E_R, are calculated as follows:

$$E_D = \frac{F_1 - F_{ss}}{\Delta l} \tag{S7}$$

$$E_R = \frac{F_{nss} - F_{ss}}{\Delta l} \tag{S8}$$

The NLRD model was used to estimate five model parameters – b, c, E_D, E_R – by minimizing the sum of squares error between the experimental and model predicted force responses using a Levenberg-Marquardt regression method.

Characteristic features of force responses to step-like length perturbations

To illustrate the characteristic features of the force responses to step-like length perturbations and to highlight the significance of the NLRD model parameters, we show a representative force response to a large-amplitude stretch (2% of ML) in Fig. S4. Upon maximal Ca^{2+} activation, the muscle fiber attains a steady-state force, F_{ss}, as a result of strong acto-myosin interactions. When the fiber is suddenly stretched in a step-like fashion, it elicits an immediate increase in force to a value, F_1, due to the rapid distortion of the elastic elements within the force-bearing XBs. The force of the muscle fiber then starts to decay rapidly due to the rapid detachment of distorted XBs and their redistribution into the non-distorted state. Following this, force begins to rise slowly due to the length-mediated recruitment of new XBs into the force-bearing state (stretch activation). Muscle force then eventually reaches a new steady-state value, F_{nss}, within a second. Stretch activation is considered to be a consequence of the length-induced recruitment of new force-bearing XBs (10-13).

The basic characteristic features of the force responses to small-amplitude stretches (0.5%, 1%, and 1.5% of ML) were symmetric to those of large-amplitude stretch (2% of ML; Fig. 1 *A* of the manuscript). However, the force responses to various amplitude quick releases were asymmetric to those of various amplitude quick stretches (Fig. 1 *A* of the manuscript). Therefore, the linear and nonlinear contractile features of the cardiac muscle fibers were demonstrated by the dependence of force response on both the amplitude, as well as the direction of the length perturbation. Linear behavior refers to the features where the amplitude of the output scales linearly with that of the input. Examples in this regard include NLRD model stiffness parameters – E_D and E_R – which scale linearly with the muscle length change (Δl). In contrast, nonlinear behavior refers to those features where the amplitude of the output does not scale linearly with that of the input. For example, NLRD model rate parameters – b and c – exhibited nonlinear trends in response to a change in ML.

Following the characteristic features of the force response illustrated in Fig. S4, the linear and nonlinear contractile features of the cardiac muscle fibers provided useful insights on various physiological phenomena that are described below.

- ***E_D***: The amplitude of instantaneous force increase (F_1) is an approximate function of the number of strongly-bound XBs and is dependent on both the amplitude of stretch and the level of Ca^{2+} activation. E_D is estimated by measuring the slope of the relationship between (F_1- F_{ss}) and Δl (see Eq. S7). Because E_D is proportional to the number of strongly-bound XBs, it represents the magnitude of stiffness increase due to the rapid distortion of the elastic elements within the strongly-bound XBs.

- ***c*:** Upon increasing to a value of F_1, force begins to decay rapidly due to the rapid detachment of the strained XBs at a dynamic rate, c. In our previous studies, we have shown that c is an approximate measure of XB detachment rate (11,12).

- ***b*:** A slow increase in the force ensues (stretch activation) at a dynamic rate, *b*. Therefore, *b* represents the rate by which additional strongly-bound XBs are recruited due to a change in ML.

- ***E_R*:** Force eventually attains a new steady-state value, F_{nss}, at the increased length. This magnitude of increase in F_{nss} is proportional to the number of newly-recruited strong XBs. Therefore, E_R is estimated as the slope of the relationship between (F_{nss}- F_{ss}) and Δl using linear regression (see Eq. S8).

Force-Velocity (F-V) measurements and estimation of maximal muscle fiber shortening velocity (V_{max})

We used a force-ramp (F-R) technique to measure the F-V relationships in detergent-skinned cardiac muscle fibers, as described previously (14). Briefly, the muscle fiber was suspended in a chamber containing pCa 9.0 solution and the SL was adjusted to either 1.9 or 2.3 µm based on a 2-D digital image corresponding to the central segment of the fiber (~ 500 µm in length). The fiber was then subjected to a maximal activation in pCa 4.3 solution and upon attainment of the steady-state, a perturbation was applied using a digital controller (model 600A, Aurora Scientific Inc., Ontario, Canada) as a linear time-dependent decrease in force i.e., a force-ramp (F-R; Fig. 2 *A* of the manuscript). The muscle fiber was allowed to continuously shorten against the force until the force on the fiber was ramped down to near zero (Fig. 2 *B* of the manuscript). The ramp rate for the F-R protocol was set to -2 F_0/sec, where F_0 represents the steady-state isometric force.

We assumed that the total force measured in activating (pCa 4.3) solution was a combination of both active (contractile element) and passive (parallel tissue) forces. Thus, in order to determine the contribution of the contractile element alone, we measured the passive forces corresponding to the exact length changes imposed during the active F-R trial and we subtracted this contribution from the total force. Fiber velocities were calculated by dividing the difference between the successive length data values with the sampling time interval. The active forces normalized with its steady state isometric value, F_0, and the shortening velocities normalized by the baseline ML, were used to construct the F-V relationship for each fiber (Fig. 2 *C* of the manuscript). Hill's hyperbolic relationship (15) was fitted to the active F-V relationships to extrapolate V_{max} as the velocity at which the net force elicited by the fiber was zero - i.e., the intercept of the F-V curve on the shortening velocity axis (indicated by *arrow* in Fig. 2 *C* of the manuscript).

SUPPORTING REFERENCES

1. Chandra, M., V. L. Rundell, J. C. Tardiff, L. A. Leinwand, P. P. De Tombe, and R. J. Solaro. 2001. Ca(2+) activation of myofilaments from transgenic mouse hearts expressing R92Q mutant cardiac troponin T. *Am J Physiol Heart Circ Physiol* 280:H705-713.

2. Chandra, M., M. L. Tschirgi, S. J. Ford, B. K. Slinker, and K. B. Campbell. 2007. Interaction between myosin heavy chain and troponin isoforms modulate cardiac myofiber contractile dynamics. *Am J Physiol Regul Integr Comp Physiol* 293:R1595-1607.

3. Fabiato, A. and F. Fabiato. 1979. Calculator programs for computing the composition of the solutions containing multiple metals and ligands used for experiments in skinned muscle cells. *J Physiol (Paris)* 75:463-505.

4. Laemmli, U. K. 1970. Cleavage of structural proteins during the assembly of the head of bacteriophage T4. *Nature* 227:680-685.

5. Chandra, M., M. L. Tschirgi, and J. C. Tardiff. 2005. Increase in tension-dependent ATP consumption induced by cardiac troponin T mutation. *Am J Physiol Heart Circ Physiol* 289:H2112-2119.

6. de Tombe, P. P. and G. J. Stienen. 1995. Protein kinase A does not alter economy of force maintenance in skinned rat cardiac trabeculae. *Circ Res* 76:734-741.

7. Stienen, G. J., R. Zaremba, and G. Elzinga. 1995. ATP utilization for calcium uptake and force production in skinned muscle fibres of Xenopus laevis. *J Physiol* 482 (Pt 1):109-122.

8. Brenner, B. and E. Eisenberg. 1986. Rate of force generation in muscle: correlation with actomyosin ATPase activity in solution. *Proc Natl Acad Sci U S A* 83:3542-3546.

9. Ford, S. J., M. Chandra, R. Mamidi, W. Dong, and K. B. Campbell. 2010. Model representation of the nonlinear step response in cardiac muscle. *J Gen Physiol* 136:159-177.

10. Linari, M., R. Bottinelli, M. A. Pellegrino, M. Reconditi, C. Reggiani, and V. Lombardi. 2004. The mechanism of the force response to stretch in human skinned muscle fibres with different myosin isoforms. *J Physiol* 554:335-352.

11. Campbell, K. B., M. Chandra, R. D. Kirkpatrick, B. K. Slinker, and W. C. Hunter. 2004. Interpreting cardiac muscle force-length dynamics using a novel functional model. *Am J Physiol Heart Circ Physiol* 286:H1535-1545.

12. Chandra, M., M. L. Tschirgi, I. Rajapakse, and K. B. Campbell. 2006. Troponin T modulates sarcomere length-dependent recruitment of cross-bridges in cardiac muscle. *Biophys J* 90:2867-2876.

13. Stelzer, J. E. and R. L. Moss. 2006. Contributions of stretch activation to length-dependent contraction in murine myocardium. *J Gen Physiol* 128:461-471.

14. Lin, D. C. and T. R. Nichols. 2003. Parameter estimation in a crossbridge muscle model. *J Biomech Eng* 125:132-140.

15. Hill, A. V. 1938. The Heat of Shortening and the Dynamic Constants of Muscle. *Proceedings of the Royal Society of London. Series B, Biological Sciences* 126:136-195.

16. Glantz, S. A. 2002. Primer of Biostatistics. New york: McGraw-Hill. 92–95 p.

SL	Functional parameter	NTG	TG
1.9 μm	pCa_{50}	5.73 ± 0.01	6.02 ± 0.01***
	n_H	3.46 ± 0.15	3.54 ± 0.18
2.3 μm	pCa_{50}	5.79 ± 0.01	6.05 ± 0.01***
	n_H	2.56 ± 0.18	1.83 ± 0.10†††

TABLE S1 Effects of the chimeric cTnT on the myofilament Ca^{2+} sensitivity (pCa_{50}) and cooperativity (n_H) of pCa-ATPase relationships. pCa_{50} and n_H were estimated by fitting the Hill's equation to the normalized pCa-ATPase data. Data were analyzed using two-way ANOVA with TnT species and SL as two factors. The TnT species-SL interaction effect on pCa_{50} was not significant, but the main effect due to TnT species was significant (*** $p < 0.001$). The TnT species-SL interaction effect on n_H was significant ($p < 0.01$), suggesting that the effect of the chimeric cTnT depended on SL. Subsequent *post hoc* multiple comparisons using Holm-Bonferroni corrected *t*-tests (16) suggested that the chimeric cTnT had a significant (††† $p < 0.001$) impact on n_H at SL of 2.3 μm, but not at 1.9 μm. Data are expressed as mean ± SE. Number of determinations was at least nine in each group. Statistical significance was set at $p < 0.05$.

Figure Legends

FIGURE S1 The composition of sarcomeric proteins in cardiac muscle preparations from NTG and TG mouse hearts. Muscle preparations were digested as described in Methods. (*A*) Standard 8% SDS-gel loaded with 25 µg of protein per sample. (*B*) Large 12.5% SDS-PAGE loaded with 300 µg of protein per sample. The gels were subsequently stained using Coomassie brilliant blue (R-250) to visualize the proteins. NTG and TG represent muscle preparations from non-transgenic and transgenic mouse hearts, respectively. MHC, myosin heavy chain; MyBP-C, myosin binding protein C; WT-cTnT, wild-type cardiac TnT; Chi-cTnT, chimeric cardiac TnT; TM, tropomyosin; cTnI, cardiac troponin I; MLC-1, myosin light chain 1; MLC-2, myosin light chain 2; cTnC, cardiac troponin C. The level of labeled sarcomeric proteins appears normal in TG cardiac muscle preparations.

FIGURE S2 Analysis of sarcomeric protein phosphorylation using Pro-Q Diamond staining. Equal quantities of digested protein samples (50 µg of protein per sample) were run on a 15% SDS-PAGE. The gel was then stained with Pro-Q diamond phosphoprotein staining solution. NTG and TG correspond to the ventricular myofibrillar preparations from non-transgenic and transgenic mouse hearts, respectively. MHC, myosin heavy chain; MyBP-C, myosin binding protein C; WT-cTnT, wild-type cardiac TnT; Chi-cTnT, chimeric cardiac TnT; TM, tropomyosin; cTnI, cardiac troponin I; MLC-1, myosin light chain 1; MLC-2, myosin light chain 2; cTnC, cardiac troponin C. Phosphorylation status of sarcomeric proteins appears similar in NTG and TG cardiac muscle preparations.

FIGURE S3 Estimation of the rate of tension redevelopment (k_{tr}). (*A*) Representative force trace (in grey) from a maximally-activated NTG fiber at SL 2.3 μm. k_{tr} was estimated by fitting a mono-exponential function to the force record, as described previously (8). F_{ss} is the steady-state isometric force and F_{res} is the residual force from which the fiber starts to redevelop force. Dashed line (in black) represents the mono-exponential fit to the experimental force record. (*B*) A representative length trace, expressed as a fraction of the muscle length, ML.

FIGURE S4 Characteristic features of the force response to 2% step-like length perturbation in NTG fiber at SL 2.3 µm. F_{ss}, initial isometric steady-state force attained by the muscle fiber in pCa 4.3 solution; F_1, the magnitude of the instantaneous force increase in response to a sudden change in the muscle length, ML; F_{nss}, new steady-state force resulting from the gradual rise in force caused by stretch activation; *b*, the rate by which new force-bearing XBs are recruited into F_{nss}; *c*, the rate by which distorted XBs dissipate and redistribute into non-distorted state, following an instantaneous change in ML.

FIGURE S5 Magnitudes of E_D and E_R in NTG and TG fibers at SL, 1.9 and 2.3 µm. Constantly-activated muscle fibers were subjected to various amplitude step-like length changes (± 0.5, ± 1.0, ± 1.5, and ± 2.0 % of initial muscle length, ML). (*A*) Instantaneous tension responses plotted against corresponding length changes in NTG and TG fibers. The slope of the relationship between ΔTension and ΔL provides an estimate of E_D (see Eq. S7). (B) New steady-state tension plotted against corresponding length changes in NTG and TG fibers. The slope of relationship between ΔTension and ΔL provides an estimate of E_R (see Eq. S8). Estimates of E_D and E_R are provided in Table 1 of the manuscript. Data are expressed as mean ± SE. Number of

determinations was at least nine in each group. Standard error bars are smaller than symbols in some cases.

FIGURE S1

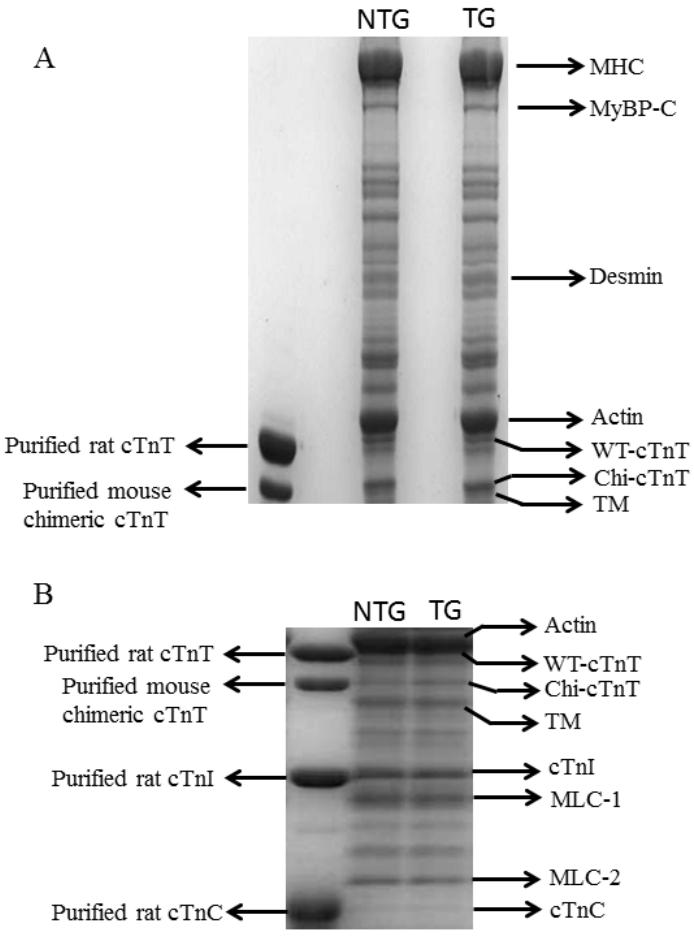
A
NTG
TG
MHC
MyBP-C
Desmin
Actin
WT-cTnT
Chi-cTnT
TM
Purified rat cTnT
Purified mouse chimeric cTnT
B
NTG
TG
Actin
WT-cTnT
Chi-cTnT
TM
cTnI
MLC-1
MLC-2
cTnC
Purified rat cTnT
Purified mouse chimeric cTnT
Purified rat cTnI
Purified rat cTnC

FIGURE S2

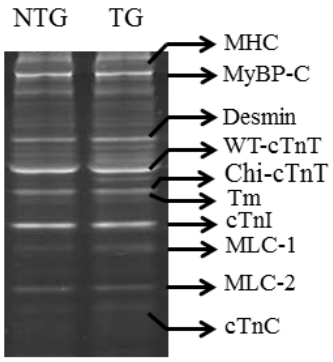
NTG
TG
MHC
MyBP-C
Desmin
WT-cTnT
Chi-cTnT
Tm
cTnI
MLC-1
MLC-2
cTnC

FIGURE S3

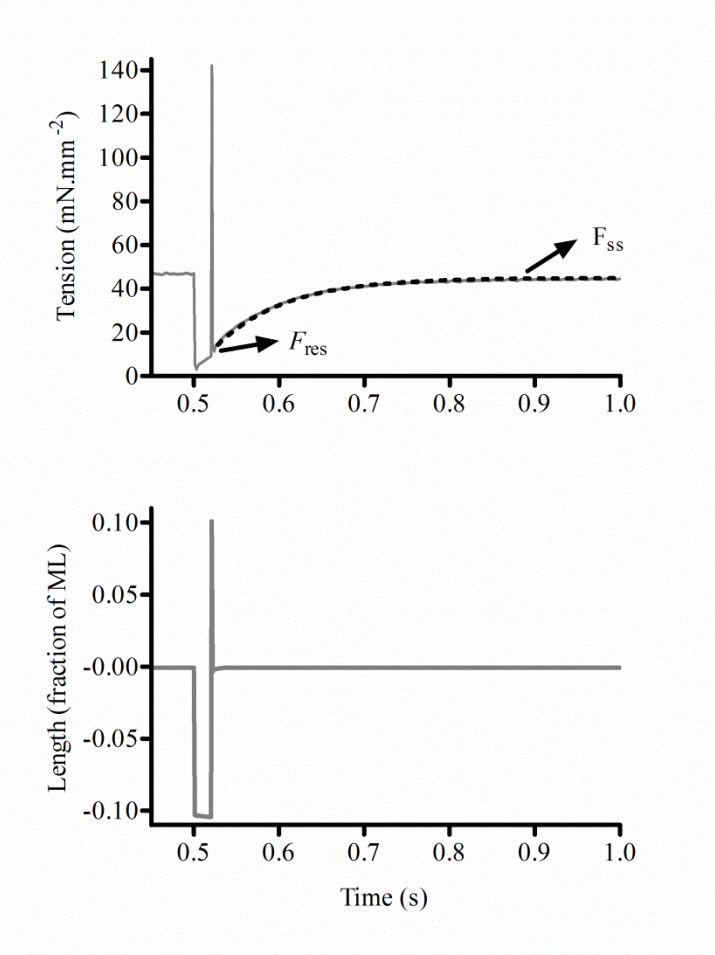
Tension (mN.mm-2)
140
120
100
80
60
40
20
0
Fss
Fres
0.5
0.6
0.7
0.8
0.9
1.0
Length (fraction of ML)
0.10
0.05
-0.00
-0.05
-0.10
Time (s)

FIGURE S4

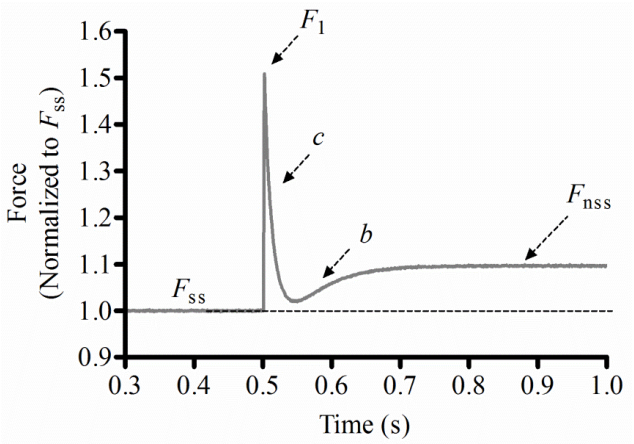
F_1
c
b
F_{nss}
F_{ss}
Force
(Normalized to F_{ss})
1.6
1.5
1.4
1.3
1.2
1.1
1.0
0.9
0.3
0.4
0.5
0.6
0.7
0.8
0.9
1.0
Time (s)

FIGURE S5

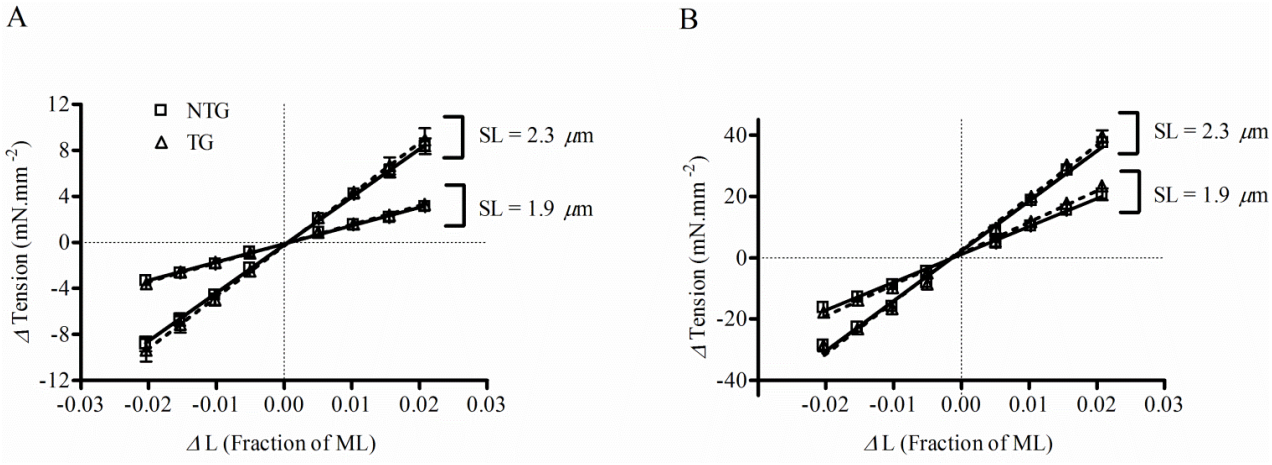
A
B
NTG
TG
SL = 2.3 μm
SL = 1.9 μm
Δ Tension (mN.mm -2)
Δ L (Fraction of ML)
12
8
4
0
-4
-8
-12
-0.03
-0.02
-0.01
0.00
0.01
0.02
0.03
40
20
0
-20
-40